

Antimony-based Quaternary Alloys for High-Speed Low-Power Electronic Devices

R. Magno^{* 1}, B. R. Bennett¹, K. Ikossi¹, M. G. Ancona¹, E. R. Glaser¹,
N. Papanicolaou¹, J. B. Boos¹, B. V. Shanabrook¹, and A. Gutierrez²

¹ Naval Research Laboratory, Washington, D.C. 20375, USA

² TRW Space and Electronics Group, One Space Park, Redondo Beach, CA 90278, USA

* Magno@bloch.nrl.navy.mil

Abstract

Heterojunction bipolar transistors using $\text{In}_z\text{Ga}_{1-z}\text{Sb}$ for the base and $\text{In}_x\text{Al}_{1-x}\text{As}_y\text{Sb}_{1-y}$ alloys for the collector and emitter have been explored. Modeling of the DC current-voltage characteristics indicate that current gain in excess of 500 may be obtained. The calculations show that the gain is a function of the base-collector conduction band offset. Molecular beam epitaxy (MBE) procedures for growing suitable alloys with a 6.2 Å lattice constant are under development. Double crystal X-ray diffraction, photoluminescence, Hall effect, and atomic force microscopy have been used to determine the quality of the materials grown. To minimize stress-induced defects, the $\text{In}_x\text{Al}_{1-x}\text{As}_y\text{Sb}_{1-y}$ alloys were grown on undoped GaSb substrates with an AlSb buffer layer. The photoluminescence data indicate that good quality $\text{In}_x\text{Al}_{1-x}\text{As}_y\text{Sb}_{1-y}$ ($x=0.52$ and $y=0.3$) with a band gap near 1 eV, is obtained using growth temperatures between 350 and 400 °C. Superior surface morphology is also found for growths in this temperature range. Te has been used to dope $\text{In}_x\text{Al}_{1-x}\text{As}_y\text{Sb}_{1-y}$ n-type in the 10^{17} cm^{-3} range. Good diode characteristics with an ideality factor of 1.1 have been obtained for $\text{In}_x\text{Al}_{1-x}\text{As}_y\text{Sb}_{1-y}$ p-n junctions grown using Te for the n-type dopant and Be for the p-type.

Introduction

InAs, AlSb, and GaSb are a group of binary semiconductors that are nearly lattice matched at 6.1 Å with a wide range of bandgaps and band offsets, as well as high electron and hole mobilities that make them desirable for use in high-speed low-power electronic devices. High electron mobility transistors^{1,2} and resonant tunneling diodes³⁻⁵ made with these binary alloys have been shown to have good operating characteristics. As part of an effort to enhance the performance of these devices and to make heterojunction bipolar transistors (HBT) in this system we have been developing MBE procedures to grow ternary and quaternary alloys with a lattice constant near 6.2 Å.⁶ In addition, we have begun to use a two dimensional model to investigate possible HBT structures.

This report focuses on the effort to develop an npn HBT with superior high-speed operating characteristics at low collector-emitter voltages to minimize power dissipation. Based on a survey of materials and band offsets a material system with a lattice constant near 6.2 Å has been chosen as a starting point. InGaSb has been chosen for the base because of its small bandgap and to exploit the good hole transport characteristics of these alloys. In

addition, it should be easy to form low-resistance ohmic contacts to InGaSb. These properties are important factors in minimizing the base resistance. Equally important is the fact that a narrow bandgap InGaSb base can be used with a collector and an emitter made from a variety of InAlAsSb alloys. While little is known about the details of the band offsets and bandgaps of these materials, extrapolations from known binary and ternary alloys indicate that it should be possible to have a large valence band offset of 300 mV or more over

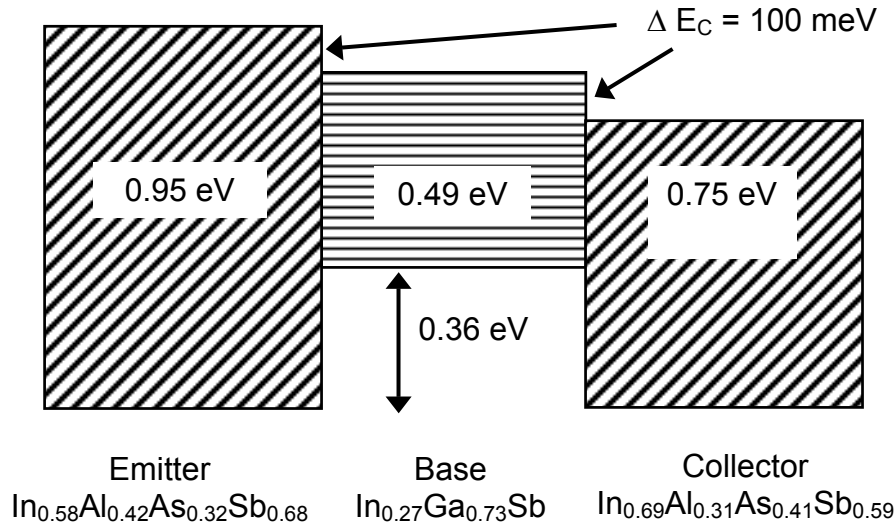


Fig. 1. An example of a possible npn HBT with an InGaSb alloy base and different InAlAsSb alloys for the emitter and collector in order to tailor the conduction band offsets at both the emitter-base and collector-base junctions.

a wide range of InAlAsSb alloys, particularly with alloys having a 6.2 Å lattice constant.^{7,8} This is important in minimizing the parasitic hole current flow from the InGaSb base to the emitter. The InAlAsSb alloys are predicted to be a direct bandgap semiconductor over a range of bandgaps from 0.2 to 1.4 eV. This leads to a wide range of possible conduction band offsets with the InGaSb base because the valence band offset is almost insensitive to the InAlAsSb composition. The above listed properties allow a great deal of latitude in using band structure engineering to optimize HBT performance. An example of the core emitter-base-collector structure of a possible HBT is illustrated in Fig. 1. A more complete picture would include other layers outside the emitter and collector region shown here. These layers would be used to obtain low resistance contacts to the emitter and collector and not considered here as this paper deals with the development of emitter-base-collector heterostructure.

Silvaco's ATLAS device simulator has been used to model HBTs composed of a variety of possible alloy combinations with the material combinations illustrated in Fig. 1 chosen as a starting point. Because of uncertainties in the material properties these calculations should be regarded as preliminary in nature and most useful for understanding the device physics and the dependences of the device characteristics on the various material

parameters. To keep things simple, a drift-diffusion model was employed with mobility

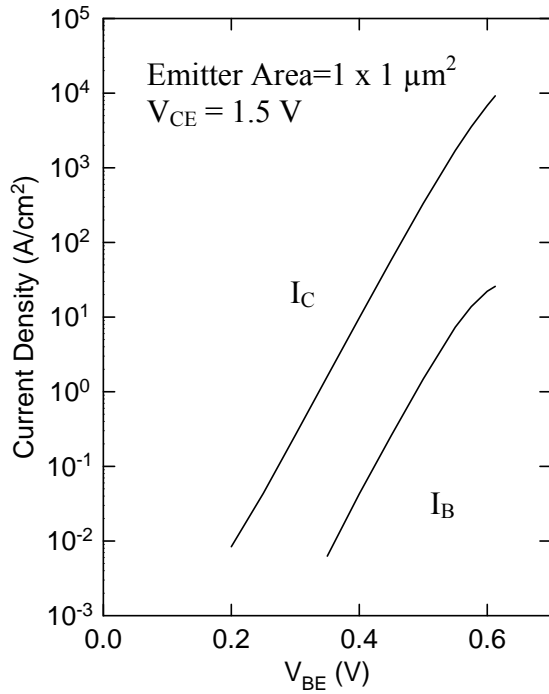


Fig. 2. Gummel characteristics for the layer structure in Fig. 1.

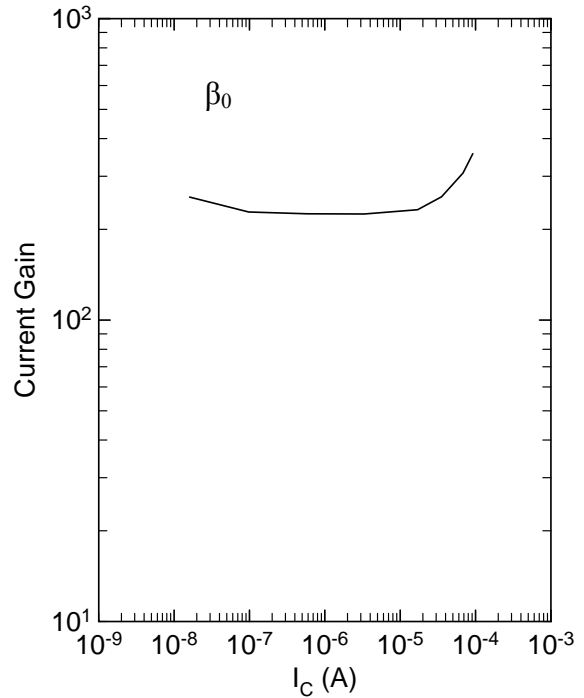


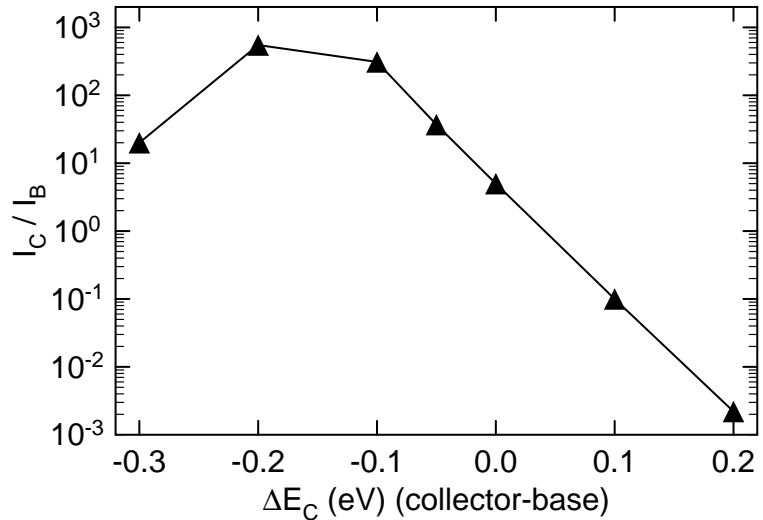
Fig. 3. DC gain obtained from I_C and I_B in Fig. 2.

models appropriate for III-V materials. Non-stationary transport effects are undoubtedly important in these devices and will be included in the future in the hydrodynamic approximation. The Gummel characteristics illustrated in Fig. 2 and the DC current gain in Fig. 3 were generated with this model for the alloy combinations in Fig. 1. The collector current in Fig. 2 is found to depend exponentially over many orders of magnitude on the emitter-base bias, and to reach a peak value over 2×10^4 A/cm². As the development of this HBT is in its infancy we consider this to be a good start as it is near 1×10^5 A/cm², the current density desirable for high frequency operation. The DC current gain found from Fig. 2 is shown in Fig. 3 to be greater than 200 and nearly constant over 4 orders of magnitude of the collector current. Fig. 4 illustrates that a DC gain greater than 500 may be obtained with the collector conduction band chosen to be 200 mV below the base conduction band. This result emphasizes that the conduction band offset between the base and collector plays a significant role in determining the DC gain, and the advantage of being able to tailor it in this material system.

The possibility of having high-performance HBTs in the antimonide materials system has led to the development of MBE methods for growing alloys like those illustrated in Fig. 1. This material system offers a vast parameter space to investigate, including the use of alloys at lattice constants other than those at 6.2 Å being investigated here. A number of problems need to be resolved in the development of the MBE growth of InAlAsSb with the

compositions of interest here. Miscibility gaps are believed to exist for these alloys that

Fig. 4. The model prediction for the dependence of the DC current gain, I_C / I_B , on the collector-base conduction band offset.

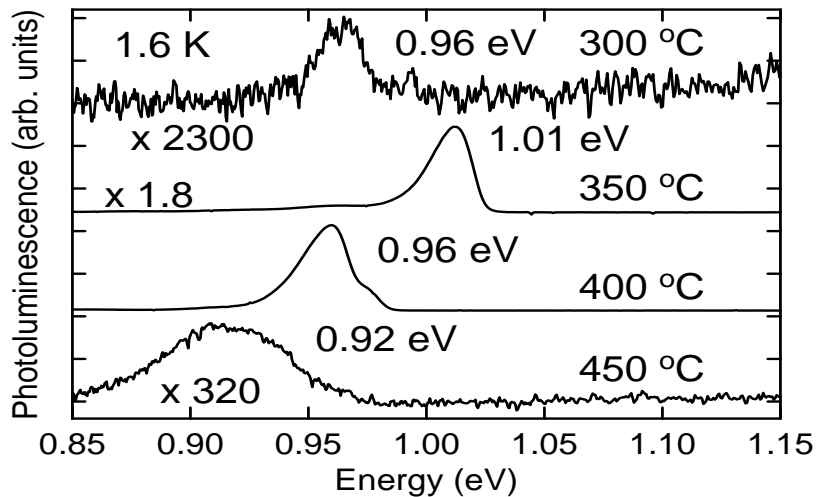


would make them difficult to grow.⁹⁻¹¹ If reasonable materials can be grown then methods need to be developed to dope them. A semi-insulating substrate is required for complex circuits, and none exist with a lattice constant near 6.2 Å. Therefore an effort needs to be made to produce either metamorphic growth procedures on semi-insulating substrates, or wafer bonding techniques.

Materials Growth

The MBE growth effort has focused on determining methods for growing good

Fig. 5. Photoluminescence measured at 1.6 K for samples grown at 300, 350, 400, and 450 °C. Each spectrum was scaled to have the same amplitude in the above plot.

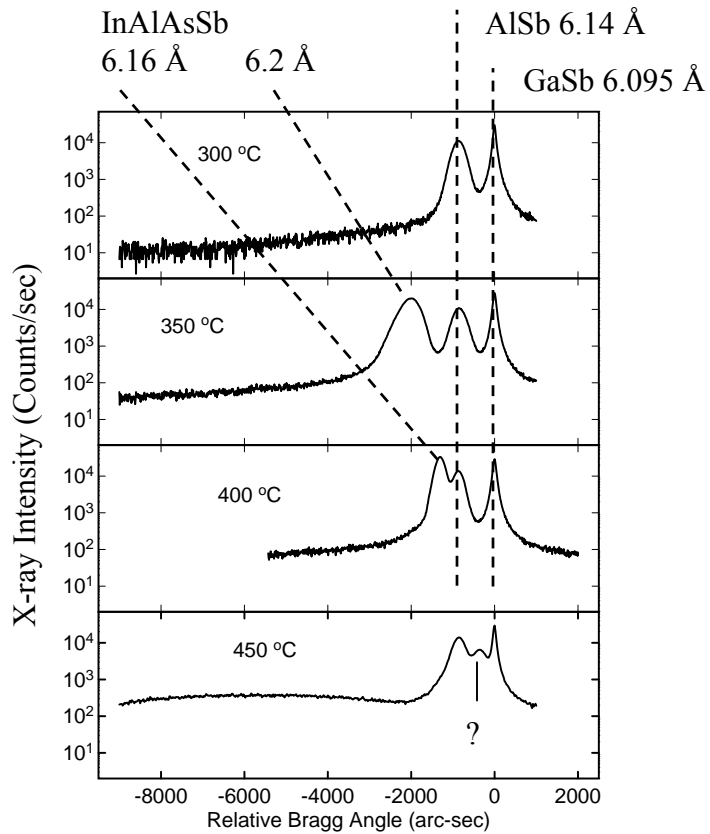


quality $\text{In}_{0.52}\text{Al}_{0.48}\text{As}_{0.25}\text{Sb}_{0.75}$ that is an alloy close to that suggested for the emitter in Fig. 1. The growth temperature, As to Sb ratio and total As plus Sb flux are parameters of concern. GaSb with a lattice constant of 6.0954 Å has been chosen as the substrate as it is

commercially available. An effort is under way to develop methods for the metamorphic growth of the desired alloys on semi-insulating InP. The growths shown below were done with a 2 μm AlSb buffer, lattice constant 6.1355 \AA , grown on an unintentionally doped GaSb substrate to accommodate part of the lattice mismatch between GaSb and the alloy at 6.2 \AA . Part of the reason for choosing a 6.2 \AA lattice constant was to minimize the mismatch with the available substrates while trying to use a narrow bandgap InGaSb base with a large valence band offset with the InAlAsSb alloys.

The growth temperature study consisted of investigating a series of $\text{In}_{0.52}\text{Al}_{0.48}\text{As}_{0.25}\text{Sb}_{0.75}$ samples at substrate temperatures of 300, 350, 400 and 450 $^{\circ}\text{C}$ while keeping the other parameters fixed. The temperature was determined by using RHEED to monitor the 5x to 3x reconstruction transition¹² after growing a few nm of GaSb on the GaSb substrate at the start of a growth. The $\text{In}_{0.52}\text{Al}_{0.48}\text{As}_{0.25}\text{Sb}_{0.75}$ layer was 2 μm thick with the first 1 μm doped with Te at $5 \times 10^{16} \text{ cm}^{-3}$ and the top 1 μm doped with Be at $1 \times 10^{18} \text{ cm}^{-3}$ to form a p-n junction. Photoluminescence (PL) measurements at 1.6 K were used to examine

Fig. 6. Double crystal X-ray diffraction for samples grown at 300, 350, 400, and 450 $^{\circ}\text{C}$.



the quality of the material and to determine the bandgap. The samples grown with substrate temperatures of 300 and 450 $^{\circ}\text{C}$ exhibited poor material quality as illustrated by the weak PL intensities in Fig. 5. Significantly more intense PL spectra are illustrated in Fig. 5 for the

samples grown at 350 and 400 °C indicating that much higher quality material is grown in this temperature range. The spread in peak energies is an indication of the variation in composition from growth to growth. Additional work needs to be done to determine whether the variations in peak energies reflect differences in the group III or V composition or a combination of both. Weak shoulders similar to the one on the high-energy side of the 400 °C spectra are often found though sometimes they are on the low energy side of the dominant peak.

The double crystal X-ray diffraction data illustrated in Fig. 6 for these samples also indicates that the best material is grown at temperatures between 350 and 400 °C. For these temperatures there are peaks in the spectra at 6.2 Å and 6.16 Å respectively due to the InAlAsSb layer. To account for both the difference in PL energy and lattice constant for the 350 and 400 °C samples requires slight differences in the Al to In ratio and the As to Sb ratio based on the predicted bandgap dependence on composition. The spectra for the 450 °C sample has a broad feature in the region corresponding to lattice constants longer than 6.2 Å, and a line near 6.1 Å that has not been found in any other samples. The X-ray data for the 300 °C sample lacks any sign of an InAlAsSb layer.

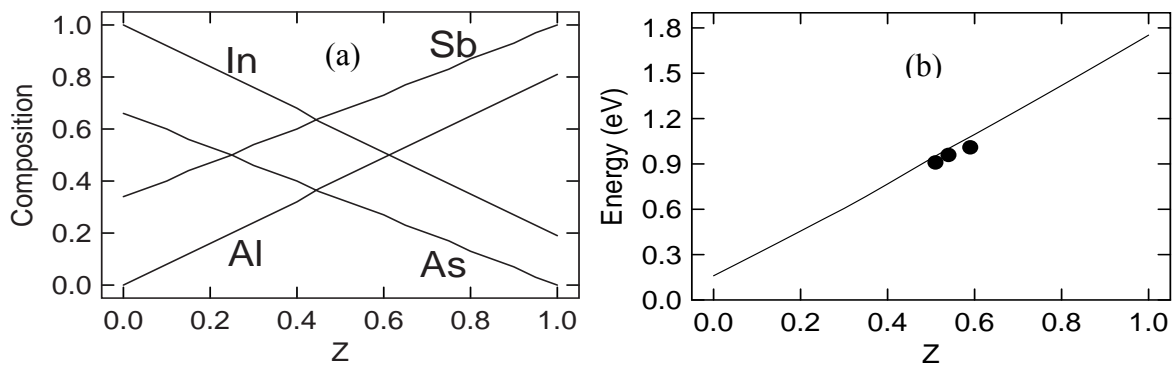


Fig. 7. (a) Dependence of composition for 6.2 Å InAlAsSb alloys on parameter, Z. (b) Comparison of the predicted dependence of the bandgap on Z, solid line, with experimental data, solid circles.

PL and X-ray measurements are not sufficient to determine the composition of these alloys. It is particularly important to know the composition in order to determine the factors controlling the incorporation of Sb and As. SIMS measurements have been performed on several samples to aid in understanding this problem, and to use with the PL data to compare the available predictions for the bandgap as a function of composition. The SIMS data gave $\text{In}_{0.53}\text{Al}_{0.47}\text{As}_{0.27}\text{Sb}_{0.73}$ for the 350 °C sample while the growth parameters were set for $\text{In}_{0.52}\text{Al}_{0.48}\text{As}_{0.25}\text{Sb}_{0.75}$. Similar variations in composition have been found for other growths. The predictions of Glisson et al.⁷ for the bandgap dependence on the composition of alloys with a 6.2 Å lattice constant have been compared with our data. To make this comparison, Glisson's composition and bandgap data have been parameterized in terms of Z as shown in

Fig. 7a, for the composition and in Fig. 7b by the solid line for the bandgap. The three black dots in Fig. 7b are experimentally determined from our data. A value of Z was found for each sample using Fig. 7a and the compositions determined by SIMS. The corresponding PL peak energies were used as a measure of the bandgaps. These three points are in reasonable agreement with the prediction represented by the solid line. Additional work needs to be done to better understand the PL mechanisms. The PL may not be due to a band-to-band recombination process, but to another process such as donor-to-acceptor, that would underestimate the bandgap energy.

Atomic force microscopy was used to measure the topography of the samples, as surface roughness is an important consideration in determining the usefulness of the material in device applications. The RMS roughness for $5 \times 5 \mu\text{m}^2$ areas is 2 nm for the 350 and 400 °C samples and 12 nm and 33 nm for the 450 and 300 °C samples, respectively. These results further support the observation that the growth window for the best quality material is between 350 and 400 °C. The surface features for the samples with 2 nm RMS were elongated and mainly aligned in one direction. Additional work needs to be done to understand the implications of this in terms of growth mechanisms and residual strain in the layers.

An npn HBT in this system requires an n-type dopant for the InAlAsSb alloys. Si is an amphoteric dopant in III-V compounds, yielding n-type conductivity in (In, Ga, Al)As but p-type in GaSb and AlSb. It was tried, but did not yield n-type material for the alloys of interest. A GaTe source was installed in the MBE to use Te for the n-type dopant.¹³ Hall effect measurements on two InAlAsSb layers indicated an electron concentration of $4 \times 10^{17} \text{ cm}^{-3}$ when grown with the GaTe cell temperature of 450 °C. This is somewhat higher than the $2 \times 10^{17} \text{ cm}^{-3}$ found for GaAs doped using the same GaTe cell temperature. The GaAs

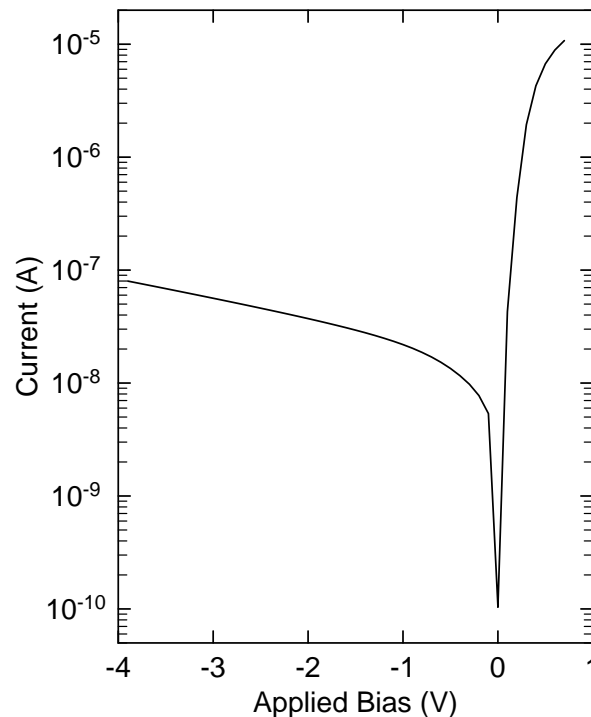


Fig. 8. Current-voltage characteristics for a mesa diode with an area of $80 \times 125 \mu\text{m}^2$ on the layer grown at 400 °C.

(Te) calibration data and the one InAlAsSb (Te) point were used to estimate the GaTe cell temperature used to dope the top layer of these samples to $5 \times 10^{16} \text{ cm}^{-3}$ to form p-n junctions.

Optical lithography and wet chemical etching were used to define mesa diodes on the at $400 \text{ }^\circ\text{C}$ is illustrated in Fig. 8. The ideality factor of 1.1 found for this data indicates a good quality diode. The slight turn over at high currents for positive bias is due to series resistance effects, due in part to the poor ohmic contact to the InAlAsSb layer. I-V probe measurements of the Be doped top layer indicate that the contacts to this layer have a low resistance and is not a significant problem here. At a reverse bias of 4 V, the leakage current density of $1 \times 10^{-11} \text{ A/cm}^2$ also indicates a good quality p-n junction, particularly considering it has a very large area.

Summary

An effort to develop an InAlAsSb/InGaSb HBT for low-power, high-speed operation has been described. Preliminary simulations indicate that the DC current gain is a function of the base-collector conduction band offset, and that gains as high as 500 are possible. Present knowledge of the bandgaps and band offsets indicate that the alloy compositions can be tuned to obtain the desired offsets and bandgaps. MBE techniques for growing the desired alloys are being developed. The substrate temperature during growth is an important factor, and a growth window has been found. SIMS data indicate that the compositions are close to those intended by the growth parameters. They are also proving to be useful in determining the limits in variation of the composition that can be tolerated in order to obtain reproducible lattice constants and bandgaps. The SIMS composition and PL data are in reasonable agreement with predictions made by extrapolating from known binary and ternary data. AFM topography measurements have found the RMS surface roughness to be 2 nm. This is another measure of the good quality of the material. Understanding the details of the surface morphology is expected to be a useful tool in understanding the growth mechanisms and the amount of residual strain at the surface.

InAlAsSb p-n junctions have been formed using Te as the n-type dopant and Be as the p-type dopant. Lithographic and wet etch procedures are under development, and have been successfully applied to form mesa diodes for I-V tests. The best I-V characteristics with an ideality factor of 1.1 and low reverse-bias leakage current have been found for material grown near $400 \text{ }^\circ\text{C}$.

Future work toward improving the quality of the InAlAsSb will involve investigating the dependence on the As and Sb fluxes and flux ratios. Preliminary work also indicates that there are better buffer layers than the AlSb when growing on GaSb substrates. InGaSb layers are being grown in an effort to improve the quality of the material needed for the HBT base. As soon as the InGaSb growth has been optimized, p-n heterojunctions will be formed, and an effort to determine the band offsets will begin. The modeling has demonstrated that this is an important parameter in device operation. The segregation and diffusion of dopants at the interfaces may also be a difficulty that needs to be addressed.

Acknowledgement

This work was supported by the Defense Advanced Research Projects Agency, and the Office of Naval Research.

The authors would like to thank Donald Sawdai, Cedric Monier, and Mike Wojtowicz for their useful discussions.

References

1. J. B. Boos, W. Kruppa, B. R. Bennett, D. Park, S. Kirchoefer, R. Bass, and H. B. Dietrich, *IEEE Trans. on Electron Devices*, **45** (9), 1869-1875, (1998).
2. J. B. Boos, B. R. Bennett, W. Kruppa, D. Park, J. Mittereder, R. Bass, and M. E. Twigg, *J. Vac. Sci. Technol. B*, **17** (3), 1022-1027, (1999).
3. J. R. Söderström, D. H. Chow, and T. C. McGill, *Appl. Phys. Lett.* **55**, 1094 (1989).
4. R. Magno, A. S. Bracker, B. R. Bennett, *J. Appl. Phys.* **89**, 5791 (2001).
5. P. Fay, J. Lu, Y. Xu, G. H. Bernstein, D. H. Chow, and J. Schulman, *IEEE Trans. On Electron Devices* **49**, 19 (2002).
6. R. Magno, B. R. Bennett, K. Ikossi, E. R. Glaser, N. Papanicolaou, J. B. Boos, and B. V. Shanabrook, 2002 Electronics Materials Conference, Univ. of California Santa Barbara, 26-28 June, 2002.
7. T. H. Glisson, J. R. Hauser, M. A. Littlejohn, C. K. Williams, *J. Electron. Mat.* **7**, 1 (1978).
8. I. Vurgaftman, J. R. Meyer, and L. R. Ram-Mohan, *J. Appl. Phys.* **89**, 5815 (2001).
9. G. B. Stringfellow, *J. Cryst. Growth* **58**, 194 (1982).
10. H. K. Choi, G. W. Turner, M. J. Manfra, and M. K. Connors, *Appl. Phys. Lett.* **68**, 2936 (1996).
11. G. W. Turner, M. J. Manfra, H. K. Choi, and M. K. Connors, *J. Cryst. Growth* **175/176**, 825 (1997).
12. M. J. Yang, W. J. Moore, C. H. Yang, R. A. Wilson, B. R. Bennett, and B. V. Shanabrook, *J. Appl. Phys.* **85**, 6632 (1999).
13. G. W. Turner, S. J. Eglash, and A. J. Strauss, *J. Vac. Sci. Technol. B* **11**, 864 (1993).